Available online at www.sciencedirect.com

ScienceDirect

Procedia Structural Integrity 1 (2016) 126–133

Structural Integrity Procedia

www.elsevier.com/locate/procedia

XV Portuguese Conference on Fracture, PCF 2016, 10-12 February 2016, Paço de Arcos, Portugal

Assessment of the fatigue life on functional hybrid laser sintering steel components

J.A.M. Ferreira[a,*], L.M.S. Santos[a], J. da Silva[a], J.M. Costa[a], C. Capela[a,b]

[a]*CEMUC, Mechanical Engineering Department, University of Coimbra, Rua Luís Reis Santos, 3030-788 Coimbra, Portugal*
[b]*Mechanical Engineering Department, ESTG, Polytechnic Institute of Leiria, 2400-901 Leiria, Portugal*

Abstract

Click here and insert your abstract text. The construction of hybrid parts: comprised of two different materials or obtained by two distinct technological processes is one of the main advantages of laser sintering metal. Various important aspects strongly affect the mechanical properties of sintering metal components: porosity, surface roughness, scan speed, layer thickness, and residual stresses. A major drawback is the occurrence of pores originating from initial powder contaminations, evaporation or local voids after powder-layer deposition, once these pores can act as stress concentrators leading to failure, especially under fatigue loading. The purpose of present work was to study the effect scan speed on the porosity and mechanical properties. Also the performance of two different material parts was studied. The sintering laser parts were manufactured in maraging steel AISI 18Ni300, while the substrates of hybrid specimens were produced alternatively in two materials: the steel for hot work tools AISI H13 and the stainless steel AISI 420.

The results showed that a very high scan speed (400 or 600 mm/s) causes the appearance of high porosity percentages and consequent drastic reduction of tensile strength and stiffness. Tensile properties of sintered specimens and two different material parts was similar. However, the fatigue strength of two different material parts tends to decrease, for long lives, when compared with single sintered specimens.

Peer-review under responsibility of the Scientific Committee of PCF 2016.

Keywords: Laser sintering metal, Fatigue, Functional materials, Mechanical properties;

* Corresponding author. Tel.: +351 239790755; fax: +351 239790701.
E-mail address: martins.ferreira@dem.uc.pt

Copyright © 2015 The Authors. Published by Elsevier B.V. This is an open access article under the CC BY-NC-ND license (http://creativecommons.org/licenses/by-nc-nd/4.0/).
Peer review under responsibility of the Scientific Committee of PCF 2016.
10.1016/j.prostr.2016.02.018

1. Introduction

Direct Metal Laser Sintering (DMLS) is a rapid manufacturing technology where a high power laser is used to fuse metallic powder particles, doing a scan of the transversal cross sections of the final component generated from a CAD model. After each scan a new powder layer is deposited and is subsequently laser sintered, until the entire component is manufactured. DMLS products could show characteristic cast structure, with high superficial roughness, presence of porosity, heterogeneous microstructure and thermal residual stresses, resulting in mechanical properties which can be improved by additional post-processing treatments. Since DMLS can be used to manufacture functional components, it is essential a good characterization of the sintered parts to control final integrity of the parts, and to warranty that the components fulfill final functional requirements. This technique is increasingly used in automotive, aerospace, medical and of injection molds industries, to obtain components with complex shapes.

The scientific and technical aspects of sintered microstructure on the mechanical properties have not been well studied and understood. DMLS sintered materials are usually anisotropic and heterogeneous (Khaing et al. (2001) and Simchi et al. (2006)), which affects the quality and performance of built parts. Earlier studies mainly focused on the influence of sintering parameters and selection of metal powder on microstructure of the sintered parts. Scarce information has been published on fatigue properties of laser sintered materials (Wang et al. (2006) and Leuders et al. (2013)) and particularly thermal fatigue (Wang et al. (2009)). Thermal fatigue cracking (or heat checking) is one of the most important failure mechanisms in hot working applications. The main reason for heat checking is rapid alternation of surface temperature, which induces high stresses enough to impose an increment of plastic strain (Persson et al. (2004)).

Various important aspects strongly affect the mechanical properties of sintered components, such as: the porosity, surface roughness, scan speed, layer thickness, and residual stresses. Internal stresses resulting from steep temperature gradients and the high cooling rates during the processing need also to be taken into account when evaluating the performance of parts manufactured from any metallic powder using selective laser melting process (Shiomi et al. (2004)). A major drawback is the occurrence of pores originating from initial powder contaminations, evaporation or local voids after powder-layer deposition (Murr et al. (2010), Gorny et al. (2011)), Brandl et al. (2012) and Vilaro et al. (2011)). Eventually, these pores act as stress concentrators leading to failure, especially under fatigue loading (Brandl et al. (2012)). At the moment these pore-like defects cannot be totally avoided, but with hot isostatic pressing (HIP) the reduction of pore size or even the closure of these can be achieved (Santos et al. (2004)).

Laser sintering metal originally destined for rapid prototyping has recently been used in the manufacture of metallic structural components. Also, the construction of hybrid parts: comprised of two different materials or obtained by two distinct technological processes is one of one the main advantages of this technique. The key idea of this project is to evaluate the parameters of the process in order to perform hybrid functional parts with optimized mechanical properties.

2. Materials and testing

Tensile static and fatigue tests were performed in round specimens with the geometry and dimensions shown in Fig. 1. Two types of samples were used: single sintered specimens (all specimen is done by laser sintering technique) and two materials hybrid samples, in which one part in made laser sintered steel and other part is a substrate machined in other steel (as shown schematically in Fig.1). The sintering laser parts were manufactured in maraging steel AISI 18Ni300, while the substrates of hybrid specimens were produced alternatively in two materials: the steel for hot work tools AISI H13 and the stainless steel AISI 420. Table 1 shows the chemical composition of the three materials, according with the manufacturers. Table 2 shows the material design composition of the three types of samples used in present study.

The samples were synthesized by Lasercusing®, with layers growing towards the application of load on the mechanical tests. The equipment for sintering is of the mark "Concept Laser" and model "M3 Linear". This apparatus comprises a laser type Nd: YAG with a maximum power of 100 W in continuous wave mode and a wavelength of 1064 nm. The samples were manufactured using the sintering scan speeds: 200, 400 and 600 mm/s.

The test series are identified by the sample code followed by the scan speed, for example ST/SS200, which means that is an hybrid specimen made one part in laser sintered steel with a scan speed of 200 mm/s and other part machined in stainless steel.

Table 1. Chemical composition of the materials.

Steel	C	Ni	Co	V	Mo	Ti	Al	Cr	P	Si	Mn	Fe
18Ni300	0.01	18.2	9.0	-	5.0	0.6	0.05	0.3	0.01	0.1	0.04	Balance
1.2344	0.40	-	-	0.94	1.30	-	-	5.29	0.017	1.05	0.36	Balance
1.2083	0.37	-	-	0.17	-	-	-	14.22	0.021	0.64	0.37	Balance

Table 2. Samples materials design.

Sample design	Sample code	Material A	Material B
Sintered	ST	18Ni300	18Ni300
Hybrid	ST/HS	18Ni300	H13
Hybrid	ST/SS	18Ni300	AISI 420

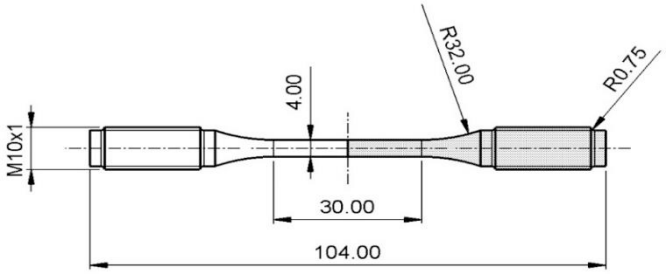

Fig. 1. Geometry and dimensions of the specimens.

The fatigue tests were carried out in tension at room temperature using a 10 kN capacity Instron Electropuls machine, at constant amplitude sinusoidal load wave was applied with a frequency within the range 15–20 Hz and stress ratios of R = 0. Tensile tests were performed with the same machine at room temperature using a testing speed of 2 mm/min.

3. Results and discussion

3.1. Metallography, porosity and micro-hardness

Cross and long sectioning of the samples in planes perpendicular and parallel to the specimen direction were prepared for metallographic analysis in order to identify the microstructure of different zones, as well as the presence of porosity.

The samples were prepared according to standard metallographic practice ASTM E407-99. To observe the microstructure of the entirely sintered steel samples it was performed a chemical attack Picral (picric acid solution 4% in ethyl alcohol) for two minutes. For the observation of all the other material formulations it was added 1% hydrochloric acid to the mixture of Picral and then it was carried out a second attack immersing the samples for 20 seconds. After prepared, the samples were observed using the microscope Leica DM4000 M LED.

Detailed images of microstructures were obtained in the sintered material and in interface region of hybrid biomaterial parts. Figs. 2 (a) and (b) show metallography in longitudinal sections of single sintered, for 200 and 400 mm/s scan speed, respectively, in which it is not noticeable a significant difference in the size and shape of grains for different scan speed. However, it is all too evident a significant increase of porosity with the scan rate. A more

amplified image of microstructure obtained for 400 mm/s scan speed is shown in Fig. 2(c) suggesting the existence of a significant number of small porosities and the formation of martensitic needles.

The quantification of the level of porosity is done by analyzing the images contrast between the pores and the base material in the photographs by optical microscopy using image processing software Image J. The program creates a border with a blank line and calculates the area of each of these zones. The sum of these areas gives the total porosity of the image. Table 3 shows the values of the porosity in percentage obtained for each batch.

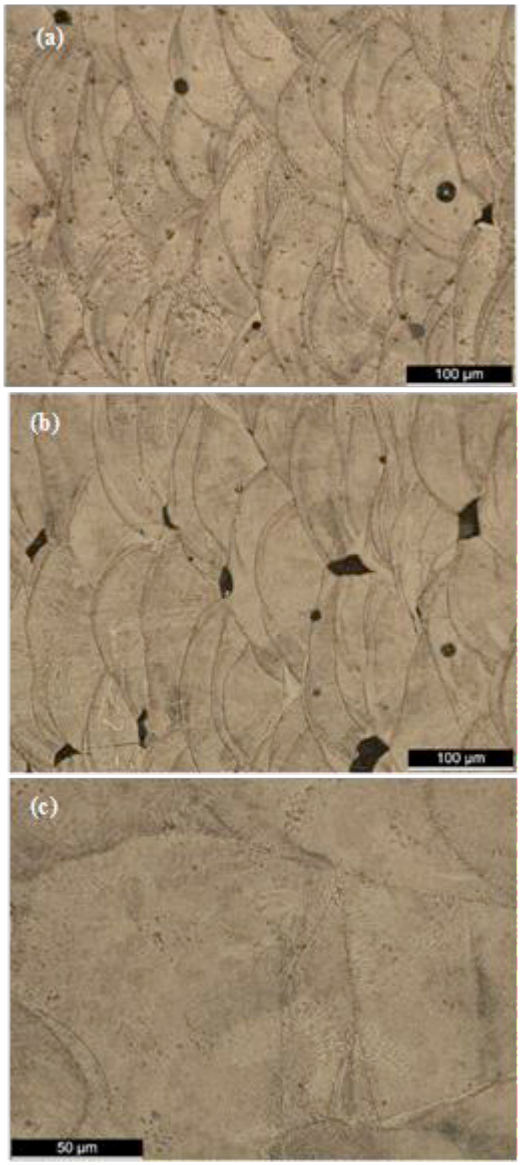

Fig. 2. Metallography's of ST specimens in longitudinal sections. Scan speeds: (a) 200 mm/s; (b) 400 mm/s; (c) 200 mm/s.

Figs. 3 shows a metallography in longitudinal section for a ST/SS200 hybrid specimen in interface region. The substrate material has a corrugated region caused by melting in the first laser pass. In AISI 420 steel it is observed a black zone which seems to indicate a higher concentration of carbon and the zone near the interface is white ferrite region showing a significant decarburization.

Vickers hardness testing was performed according to ASTM E384-11e1 using a Struers Duramin 1 microhardness tester with a 1.0 kg load and 0.5 mm between indentations. In interface region distance between indentations was 0.25 mm. For single sintered specimens measurements were randomly done in longitudinal sections, and the values of average and standard deviations are also indicated in Table 3. Increasing the scan speed produces only a slight reduction in hardness and an increase in dispersion. For hybrid specimens, hardness was measured along a longitudinal line in longitudinal sections, and the obtained values are shown in Fig.4. Microhardness of sintered region was significantly lower in sintered region than in substrate, in about 35% and 29% for AISI 420 and AISI H13, respectively.

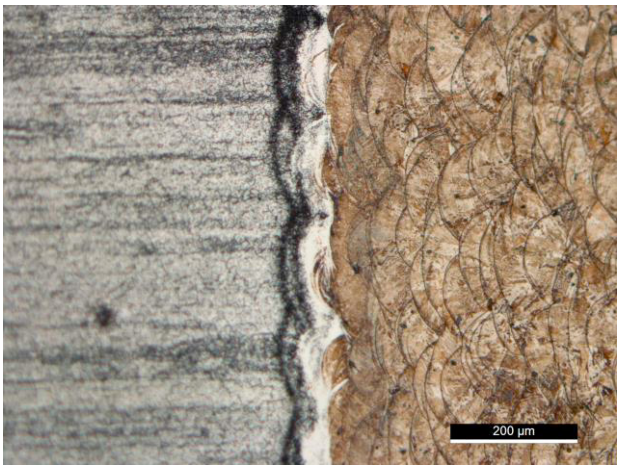

Fig. 3. Metallography in longitudinal section for a ST/SS200 hybrid specimen.

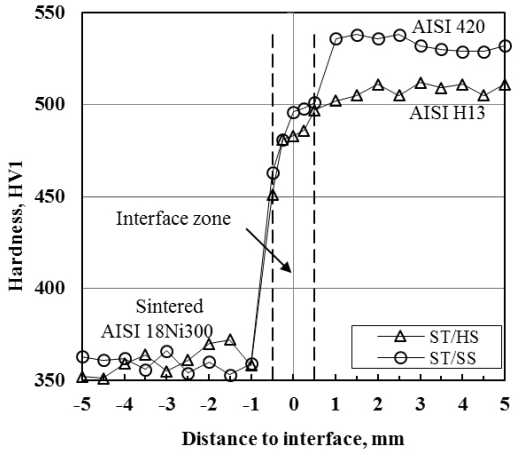

Fig. 4. Microhardness profile for a ST/SS200 hybrid specimen.

3.2. Mechanical properties

Fig. 5 shows representative load–displacement curves obtained for single sintered specimens for different scan speeds. The typical metallic behaviour showing an initial linear region followed by a non-linear behaviour was observed. The increasing of the sintering scan speed was associated to an increasing of porosity level causing drastic reduction of the ultimate stress and of the Young`s modulus.

Ultimate strength was calculated as the maximum stress obtained using peak load of the load versus displacement curves. The stiffness modulus was obtained by linear regression of the stress-strain curves considering the larger

range corresponding to a correlation coefficient higher than 0.995%. Table 3 also summarizes the mechanical properties obtained for single sintered specimens for different scan speeds and for hybrid parts.

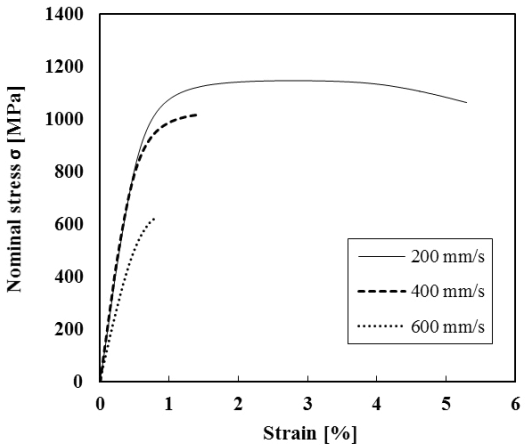

Fig. 5. Exemplary tensile curves.

Table 3. Mechanical properties.

Sample code	Scan speed, mm/s	Porosity %	Hardness HV1	Young`s Modulus, GPa	Tensile Strength, MPa	Strain at failure, %
ST	200	0.74±0.09	354±5	168±29	1147±13	5.12±0.001
	400	7.37±0.99	348±6	155±30	1032±27	1.45±0.01
	600	10.38±2.88	341±8	104±38	612±22	0.71±0.002
ST/HS	200	-	-	181±6	1139±12	4.6±0.03
	400	-	-	163±9	1001±5	1.7±0.001
ST/SS	200	-	-	163±7	1144±10	4.9±0.08
	400	-	-	138±18	990±17	1.38±0.002

3.3. Fatigue results

The fatigue results obtained under pulsating tensile loading, analysed in terms of the stress range against the number of cycles to failure, are depicted in Fig. 6 for single sintered material and the two types of hybrid biomaterial parts. All the three samples batches were manufactured with 200 mm/s scan speed. The analysis of the figure indicates that for short lives fatigue strength of the three combinations of materials is similar. However, for longer life, the fatigue strength of hybrid specimens are progressively less than that of the fully sintered samples achieving a reduction in the order of 30% for N = 5x105 cycles. It required further examination for a convincing justification for these results.

Finally, a fracture surface analysis was performed with a scanning electron microscope (Philips XL30). Fig. 7 shows three exemplary SEM images. The fracture surface analysis showed that the crack initiated on the specimens surface, in all treatments and specimens, and propagated through the cross section. In many cases it was observed a multi-nucleation as shown in Fig. 7a). Brittle crack propagation was the main mechanism observed in all cases. Fig. 7b) is a representative image, showing the initiation at the surface and the brittle crack propagation. Fig. 7c) is a more magnified image that stands out brittle fracture as the main failure mechanism. Fig. 7a) is a low magnification image which reveals the texture of the cross section of the sintered test pieces, ie the shape and orientation of the grains deposited in each layer. The morphology shown in Fig. 7a) suggests that the intergranular fracture mode occurs between the deposited layers.

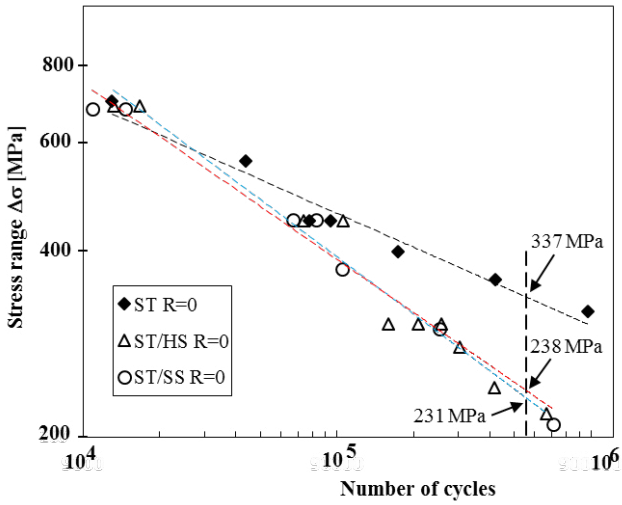

Fig. 6. S-N curves.

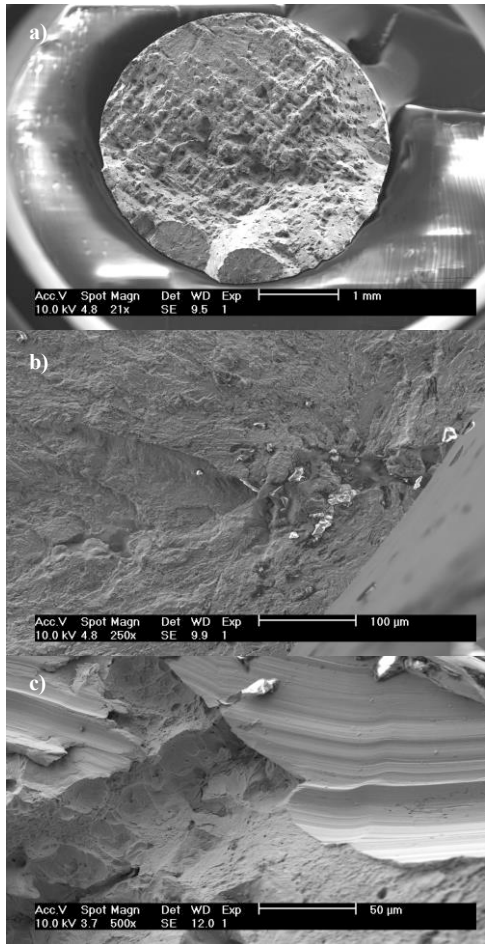

Fig. 7. SEM observations. a) Multi-nucleation; b) Initiation at the surface; c) Brittle fracture.

4. Conclusions

Present work studied the static and fatigue response of single laser sintered specimens and two materials hybrid formulations. The main conclusions are:

- Very high scan speed (400 or 600 mm/s) causes high porosity percentages and consequent drastic reduction of tensile strength and stiffness;
- Tensile properties of single laser sintered parts and two materials hybrid parts were quite similar;
- Fatigue strength of hybrid parts is quite similar to that of single sintered specimens for short lives, but tends to became significant lower for long lives, reaching about 30% for N = 5x105 cycles.

Acknowledgements

This research is sponsored by FEDER funds through the program COMPETE (under project T449508144-00019113) and by national funds through FCT – Fundação para a Ciência e a Tecnologia –, under the project PTDC/EMS-PRO/1356/2014. The authors would like to acknowledge also EROFIO, Batalha, Portugal for the supply of materials and samples used in this project.

References

Brandl, E., Heckenberger, U., Holzinger, V., Buchbinder, D., 2012. Additive manufactured AlSi10Mg samples using selective laser melting (SLM): microstructure, high cycle fatigue, and fracture behaviour. Mater Design 34, 159–69.

Gorny, B., Niendorf, T., Lackmann, J., Thöne, M., Tröster, T., Maier, H.J., 2011. In situ characterization of the deformation and failure behaviour of non-stochastic porous structures processed by selective laser melting. Mater Sci Eng A528 (27), 962-967.

Khaing, M.W., Fuh, J.Y.H., Lu, L., 2001. Direct metal laser sintering for rapid tooling: processing and characterization of EOS parts. Journal of Materials Processing Technology 113, 269–272.

Leuders, S., Thöne, M., Riemer, A., Niendorf, T., Tröster, T., Richard, H.A., Maier, H.J., 2013. On the mechanical behaviour of titanium alloy TiAl6V4 manufactured by selective laser melting: Fatigue resistance and crack growth performance. International Journal of Fatigue 48, 300–307.

Murr, L.E., Gaytan, S.M., Ceylan, A., Martinez, E., Martinez, J.L., Hernandez, D.H., et al., 2010. Characterization of titanium aluminide alloy components fabricated by additive manufacturing using electron beam melting. Acta Mater 58(5), 1887–1894.

Persson, A., Hogmark, S., Bergström, J., 2004. Simulation and evaluation of thermal fatigue cracking of hot work tool steels. International Journal of Fatigue 26, 1095–1107.

Santos, E.C., Osakada, K., Shiomi, M., Kitamura, Y., Abe, F., 2004. Microstructure and mechanical properties of pure titanium models fabricated by selective laser melting. Proc Inst Mech Eng C, J Mech Eng Sci, 218(7), 711–719.

Shiomi, M., Osakada, K., Nakamura, K., Yamashita, T., Abe, F., 2004. Residual stress within metallic model made by selective laser melting process. CIRP Ann – Manuf Tech 53(1), 195–198.

Simchi, A., 2006, Direct laser sintering of metal powders: Mechanism, kinetics and microstructural features. Materials Science and Engineering A 428 (1–2), 148–158.

Vilaro, T., Colin, C., Bartout, J.D., 2011. As-fabricated and heat-treated microstructures of the Ti–6Al–4V alloy processed by selective laser melting. Metall Mater Trans A 42A(10), 3190–3199.

Wang, Y., Bergstrom, J., Burman, C., 2006. Four-point bending fatigue behaviour of an iron-based laser sintered material. International Journal of Fatigue 28, 1705–1715.

Wang, Y., Bergstrom, J., Burman, C., 2009. Thermal fatigue behavior of an iron-based laser sintered material. Materials Science and Engineering A 513–514, 64–71.